The Libyan Journa of Science

The Libyan Journal of Science- University of Tripoli Vol. 25, No. 01 (2022) 4-9

Study of MoO_3 doping effect on linear and Non-linear optical properties of Cellulose acetate (CA) films

Mohamed Abu. Hamza[1], Saad E. Sharada[2]

[1]University of Tripoli, Faculty of Scienc, Tripoli/Libya

[2]University of Tripoli, Faculty of Education (Qaser Bin Ghashir), Tripoli/Libya

Corresponding author: Mohamed Abu. Hamza Moham.Hamza@uot.edu.ly

ARTICLE INFO

Article history:

Received 24/05/2022

Received in revised form 02/08/2022

Accepted 07/08/2022

ABSTRACT

The goal of this study was to investigate the optical properties of the prepared CA-MoO_3 nanocomposites films. CA has been chosen as a host matrix and then doped with MoO_3 with different concentrations (2.5, 5, 10 and 15wt. %) of MoO_3 by using casting procedure. CA-MoO_3 films were characterized by UV-Visible spectrophotometer within the wavelength range of 200 nm-800 nm. The Linear optical parameters (transmission (T), extinction coefficient (K), reflectance (R), refractive index (n), real (ε_1) and imaginary (ε_2) part of the dielectric constant and optical conductivity (σ_{opt})) of CA-MoO_3 films were obtained from absorption spectra. The volume (VELF) and surface (SELF) energy loss function of CA-MoO_3 films were obtained by complex dielectric constant. The Dispersion parameters (dispersion energy (E_d), oscillation energy (E_0), static dielectric constant (ε_0) and static refractive index (n_0)) were calculated using theoretical Wemple-DiDomenico model. The nonlinear optical susceptibility $x^{(1)}$, $x^{(3)}$ and nonlinear refractive index n_2 were evaluated from the linear optical parameters using semiempirical relation. The results show that the Linear and nonlinear optical parameters change with the increase of molybdenum trioxide concentration, where, the transmittance, oscillator energy, the volume (VELF) and surface (SELF) energy loss decreases with the increase of MoO_3 concentration.

Keywords: CA; SELF; static dielectric constant; refractive index; oscillation energy.

1. Introduction

Polymer composites are important because of their valuable role in various aspects of our daily lives. Their attractive characteristics, including their low-cost, abundance, and flexibility. Most polymers are considered non-toxic and could easily play the role of host matrices for different sorts of fillers [1–8]. Improving the polymers' optical, electrical and mechanical properties can be achieved via implanted limited concentrations of fillers to match desired applications. These applications include optoelectronic devices, sensors, solar cells, capacitors, reduction of environmental pollution and ceramics [9]. Natural polymers like cellulose show a great potential for future use as an alternative for the non-biodegradable polymers their low energy consumption. Cellulose acetate (CA) in particular of all other cellulose derivatives because of its excellent optical clarity, biodegradability, and high toughness and other physical properties. CA is also largely used as a film base in photography and as a filler material in cigarettes. Due to its low cost can be used in textile, membrane technology, drug release, UV protector, Opto-electronic field and a wide range of applications in different fields. This wide range application of CA is limited by its high

moisture sensitivity and brittle nature. Studies show that to improve CA properties, nanomaterials such as graphene oxide, montmorillonite, carbon nanotubes, silver, and gold are embedded in CA matrix, can reinforce and enhance its properties effectively, such as UV shields, flame retardants, photo activity and gas permeability [10].

Transition metal oxides such as MoO_3 are semiconductor materials that have a wide technological application, in display devices, optical smart windows, Electrochromic devices, and gas sensors. MoO_3, exhibit great structural, chemical, and optical properties. It is considered as a cryogenic material because it displays electrophotochromic and gasochromic properties by virtue of which gives the material the potential for the development of electronic display devices. MoO3 film has a several application, as in sensors and lubricants, and makes it a candidate for back contact layer of cadmium Telluride solar cells [11].

In the present work, the linear optical parameters of CA-MoO_3 films have been evaluated from absorption spectra. As per author's information, first time the dispersion of refractive index and the non-linear optical parameters of CA-MoO_3 were studied using semi empirical models.

2. Experimental methods

2.1. Materials

Cellulose acetate polymer (CA) was used as starting material for preparation of films. It was purchased from Thomas Baker Lab Chemicals, India, white color and nontoxic powder has 53.5-54.5% degree of acetylation. Molybdenum trioxide (MoO_3) was obtained from Riedel-de Haen, (Germany), as a light gray powder, with a molecular weight of 143.94 g/Mol, 99.5% purity and was used without further purification. Dichloromethane compound (M.W=84.93) with a purity of 99%, and N, Ndimethyl formamide (M.W=73.9) with a purity of 99% were obtained from the Park Scientific Limited, Northampton U.K. It was used without any further purification and employed to dissolve CA and MoO_3.

2.2. Preparation of composite films

Cellulose acetate (CA) with different proportions of molybdenum trioxide (MoO_3) (2.5, 5, 10 and 15wt. %) films were prepared by solution casting technique. In this process, one gram of CA was dissolved in the volume ratio of (25:1) dichloromethane: N, N-dimethyl formamide. The mixture is placed on a magnetic stirrer to complete the solubility with continued stirring at room temperature. An exact weight of MoO_3 based on the weight of CA was added to the solution of CA. After MoO_3 completely dissolved in CA solution, the mixture was poured into a flat bottom glass container prior to prepare the film. The glass container was covered and placed on a flat bench to evaporate both dichloromethane and N, N-dimethyl formamide solvent.

2.3. Optical characterization

A UV–visible spectrophotometer (Lambda 25, Perkin Elmer) was utilized to record the absorbance (A) and transmittance (T) spectra of the prepared samples over the scanned wavelength range 200–800 nm at room temperature. Based on the measured A and T data, the extinction coefficient (K), refractive index (n), reflectance (R) and the optical conductivity (σ_{opt}) values of the prepared composites were determined using the following equations [12–19]:

$$k = \frac{\alpha\lambda}{4\pi} \quad (1)$$

$$n = \frac{1+\sqrt{R}}{1-\sqrt{R}} + \sqrt{\frac{4R}{(1-R)^2} - K^2} \quad (2)$$

$$R = 1 - \sqrt{T - e^{A}} \quad (3)$$

$$\sigma_{op} = \frac{\alpha nc}{4\pi} \quad (4)$$

Where (α) is the absorption coefficient, (c) is the speed of light in a vacuum and (λ) is the wavelength of the incident light.

The fundamental electron excitation spectra of CA-MoO_3 films are described with complex dielectric constant. The real part of dielectric constant is related to the property of slowing down the speed of light in the materials. Whereas, the imaginary part of dielectric constant is related with the absorbing energy from electric field due to dipole motion. The value of real and imaginary part of dielectric constant was obtained from the following formula; [20]:

$$\varepsilon = \varepsilon_1 + \varepsilon_2 \quad (5)$$

Where

$$\varepsilon_1 = n^2 - k^2 \quad (6)$$

$$\varepsilon_2 = 2nk \quad (7)$$

The energy dispersion parameter of refractive index can be evaluated from the supposed Wemple and DiDomenico (WDD) single-oscillator model according to the following equation [21]:

$$(n^2-1)^{-1} = \frac{E_0}{E_d} + \frac{1}{E_0 E_d}(h\nu)^2 \qquad (8)$$

Where E_0 is the average value of the single oscillator energy of the electronic transitions, which is usually considered as an average energy gap, and E_d is the dispersion energy that measures the average strength of inter-band optical transitions. The static refractive index n_0 at a zero photon energy is determined from Eq. (9) in Ref. [22]:

$$n_0^2 = 1 + \frac{E_d}{E_0} \qquad (9)$$

The energy loss of the incident electromagnetic waves by electrons in a material or surface coating is connected with the volume energy loss function (VELF) and the surface energy loss function (SELF), respectively. Both the surface and volume energies are obtained from complex dielectric constant [23]:

$$\text{SELF} = \frac{\varepsilon_2}{(\varepsilon_1+1)^2 + \varepsilon_2{}^2} \qquad (10)$$

$$\text{VELF} = \frac{\varepsilon_2}{\varepsilon_1{}^2 + \varepsilon_2{}^2} \qquad (11)$$

Nonlinear optical parameters of materials are very useful for the fabrication of frequency conversion and optical switching devices, which in turn play an essential role in Photonics. The third order optical non-linear susceptibility gives the information about the strength of chemical bonds between the molecules of CA-MoO_3 films [24]. The linear optical susceptibility $x^{(1)}$ of the medium can be computed from the relation [25]:

$$X^{(1)} = \frac{E_d/E_0}{4\pi} \qquad (12)$$

The nonlinear third order of the optical susceptibility $X^{(3)}$ could be estimated from linear optical susceptibility by applying $X^{(1)}$ Miller's rule like the following formula [25]:

$$X^{(3)} = k\,(X^{(1)})^4 \qquad (13)$$

Where, K is constant (1.7×10^{-10} esu).

3. Results and discussion

From the transmittance spectra Figure 1, it can be observed that the transmittance decreases as the doping wt% is increased.

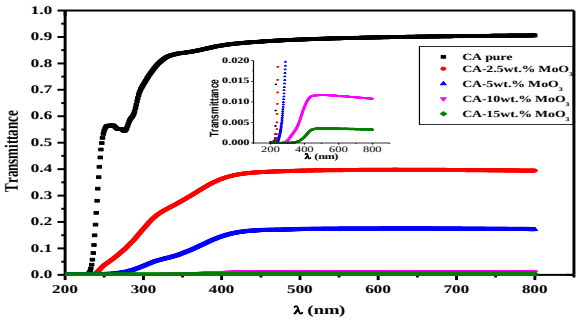

Fig.1. The transmittance spectra for CA-MoO_3 films as a function of incident wavelength.

Figure 2 presents the variations of extinction coefficient (k) with the wavelength for pure CA and CA-MoO_3 composite films. It can be seen that the value of k increases with MoO_3 weight percentage increase. The increase of the extinction coefficient for the electrolyte films with MoO_3 concentration is due to the increase in the absorption coefficient [26]. This result indicates that the doping of MoO_3 tends to change the optical properties of the host polymer.

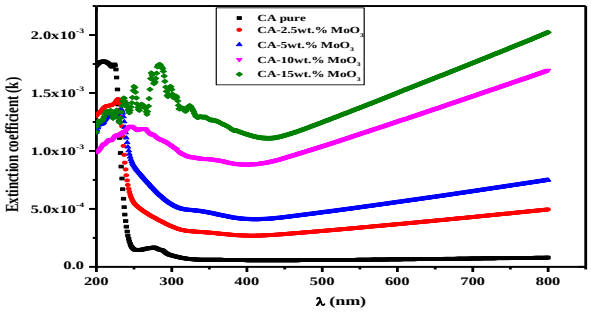

Fig.2. The variation of the extinction coefficient (k) with wavelength of the CA and CA- MoO_3 composite films.

The reflectance increases with an increase in the concentration of the doped MoO_3 nanoparticles; see Figure 3.

Figure 4 displays the increase in refractive index of the doped MoO_3 films with increasing the content of MoO_3 nanoparticles, with respect to pure CA. It is observed also that the refractive index reduced at higher energy (shorter wavelength), which suggests the behavior of the normal dispersion of the material in the visible range [27,28].

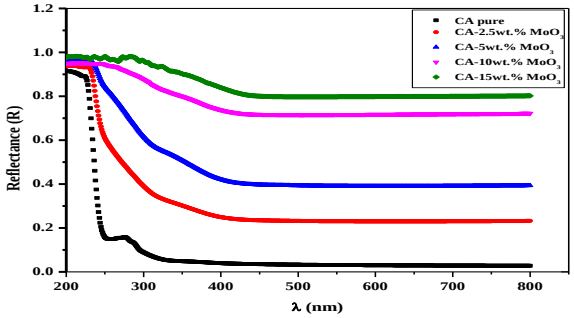

Fig.3. The reflectance of CA and CA-MoO_3 films as a function of wavelength.

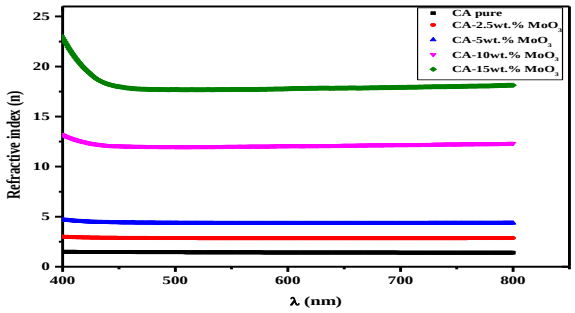

Fig.4. The refraction index of prepared films as a function of wavelength.

Figure 5 shows the variation of optical conductivity of the CA - MoO_3 with the wavelength of the incident photon. It is clear that the optical conductivity of the films increases with the increase in MoO_3 weight percentage. This increase can be attributed to the creation of new energy levels in the band gap which facilitate the crossing of electrons from the valence band to these local levels, then to the conduction band and, consequently, the band gap decreases and the conductivity increases [29].

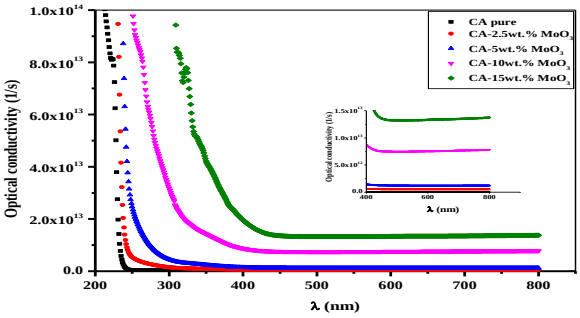

Fig.5. The optical conductivity of the prepared films as a function of incident wavelength.

The values of E_0 and E_d were calculated by plotting $(n^2-1)^{-1}$ versus $(h\nu)^2$ as shown in Figure 6. The plots give straight lines which intercept *y*-axis in a value equal to (E_0/E_d), and the slope equal to $(-1/E_0E_d)$. The evaluated values of E_0 and E_d are recorded in Table 1. It is obvious that the single-oscillator energy, E_0 values decrease with increasing MoO_3 content and E_d values were enhanced by increasing the MoO_3 concentration. The increase in the dispersion energy (E_d) indicates the increase in bond strength, which leads to increase in the degree of disorder [21].

The computed values of the static refractive index (n_0) and the static dielectric constant ($\varepsilon_0 = n_0^2$) are listed in Table.1 which were enhanced with the concentration of MoO_3 nanoparticles.

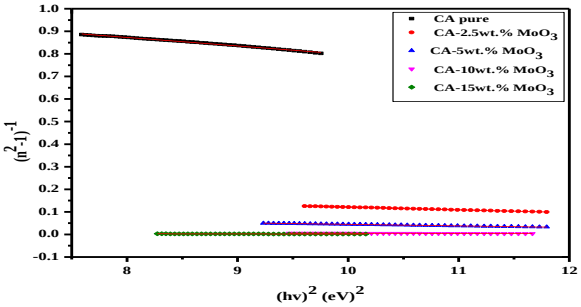

Fig.6. The relationship between $(n^2-1)^{-1}$ and $(h\nu)^2$ for CA and CA - MoO_3 films.

Table1. Single-oscillator energy, E_0, dispersion energy, E_d, static refractive index (n_0) and the static dielectric constant, ε_0, values according to Wemple and DiDomenico model.

Sample (wt%)	E_0(eV)	E_d (eV)	n_0	ε_0
0	5.58	4.75	1.36	1.85
2.5	4.47	18.47	2.27	5.15
5	4.07	36.10	3.14	9.86
10	3.90	248.4	8.04	64.64
15	3.53	403.43	10.74	115.34

The dependence of ε_1 and ε_2 on photon wavelength is shown in Figures 7 and 8. It is observed that the real part values of dielectric constant ε_1 depend more than the imaginary part of dielectric constant e2 which is due to e1 on the refractive index (*n*), on the other hand ε_2 depends on the extinction coefficient (*k*) [20]. The values of both parameters increase with the increase of the weight percentage of MoO_3 nanoparticles in the CA matrix.

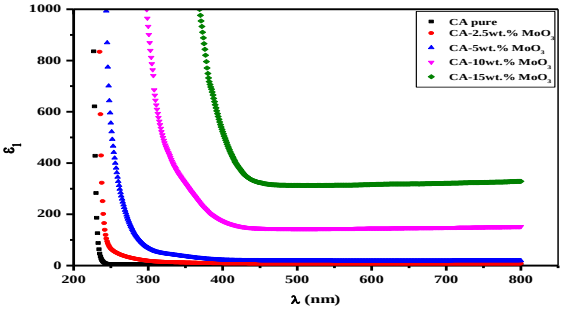

Fig.7. The real dielectric constant for CA and CA-MoO_3 composite films as a function of incident wavelength.

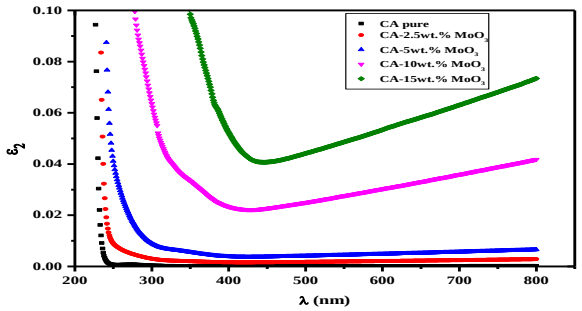

Fig.8. The imaginary dielectric constant of CA and CA-MoO_3 composites films as a function of incident wavelength.

The variations of VELF and SELF with the incident spectrum energy in the energy range of (1.5–6.5 eV) are shown in Figures 9 and 10, respectively. The VELF values are always greater than SELF values for all the samples. The VELF and SELF decreased as the MoO_3 nanoparticle concentration increased.

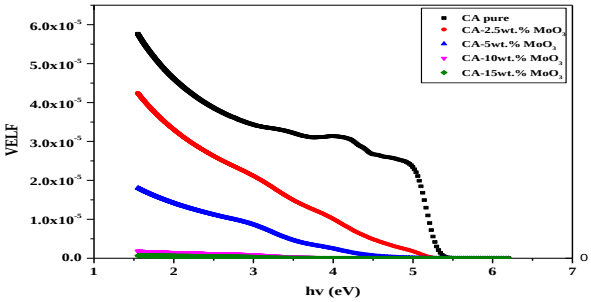

Fig.9. Variation of a VELF with the photon energy for the CA-MoO_3 nanocomposites.

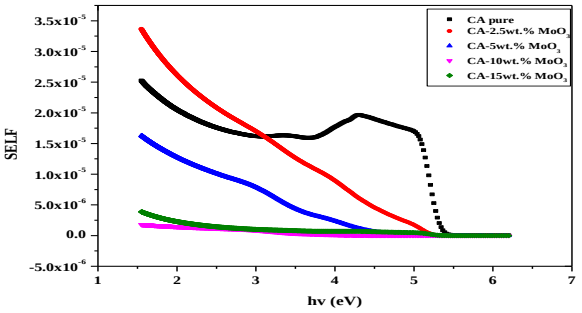

Fig.10. Variation of a SELF with the photon energy for the CA-MoO_3 nanocomposites.

The evaluated values of the linear optical susceptibility are listed in Table 2. It was found that the values of the linear optical susceptibility, nonlinear third-order optical susceptibility, and nonlinear refractive index increase as the content of MoO_3 nanoparticles increases. The high values of the nonlinear third-order susceptibility and nonlinear refractive index show the suitability of the samples to be used in different nonlinear optical and photonic devices and applications [25].

Table 2. Values of $x^{(1)}$, $x^{(3)}$, and n_2 of the prepared CA-MoO_3 nanocomposites

Sample (wt%)	$x^{(1)}$	$x^{(3)}$ (e.s.u)	n_2 (e.s.u)
0	0.0678	3.59×10^{-15}	9.95×10^{-14}
2.5	0.329	1.99×10^{-12}	3.30×10^{-11}
5	0.706	4.22×10^{-11}	5.06×10^{-10}
10	5.071	6.61×10^{-8}	3.1×10^{-7}
15	9.099	1.17×10^{-6}	4.1×10^{-6}

4. Conclusion

Linear and nonlinear optical studies were performed for pure CA and CA doped by MoO_3 with different concentrations utilizing the casting techniques. The transmittance (T) and the average values of single oscillator energy for electronic transitions (E_0) are decreasing with increasing MoO_3. The extinction coefficient (K), refractive index (n), reflectance (R) and the optical conductivity (σ_{opt}), refractive index (n), and dielectric constant (ε) increase with increasing MoO_3. Third-order nonlinear optical susceptibility $x(3)$ and the nonlinear refractive index n_2 were observed to increase with increasing the amount of MoO_3 nanoparticles.

These results indicate that the film we had prepared can be used in many applications, including anti-reflective coating, photonic devices and as a UV sensor.

5. References

[1] Badawi, A. (2021), Enhancement of the optical properties of PVP using Zn1-xSnxS for UV-region optical applications, Appl PhysA, 127:51,1-9

[2] Xiao, W., Song, J., Huang, L., Yang, Z., Qiao, Q. (2020), PVA-ZrO2 multilayer composite separator with enhanced electrolyte property and mechanical strength for lithium-ion batteries. Ceram Int, 46,29212–29221.

[3] Badawi, A.and Alharthi, SS. (2020), Controlling the optical and mechanical properties of polyvinyl alcohol using Ag2S semiconductor for environmentally friendly applications, Mater SciSemicond Process, 116, 1-8.

[4] Kabir, H., Nandyala, SH., Rahman, MM., Kabir, MA., Pikramenou, Z., Laver, M.,and Stamboulis, A. (2019), Polyethylene glycol assisted facile sol-gel synthesis of lanthanum oxide nanoparticles: Structural characterizations and photoluminescence studies, Ceram Int, 45,424–431.

[5] Badawi, A., Alharthi, SS., Mostafa, NY., Althobaiti, MG., and Altalhi, T. (2019), Effect of carbon quantum dots on the optical and electrical properties of polyvinylidene fluoride polymer for optoelectronic applications, Appl Phys A, 125,1-9.

[6] El-Zaidia, E., Ali, H., Hamdalla, T., Darwish, A., and Hanafy, T. (2020), Optical linearity and bandgap analysis of Erythrosine B doped in polyvinyl alcohol films. Opt Mater, 100,1-5.

[7] Al-Baradi, A., Al-Shehri, S., Badawi, A., Merazga, A., and Atta, A. (2018), A study of optical, mechanical and electrical properties of poly (methacrylic acid) /TiO2 nanocomposite, Results Phys, 9, s879–885.

[8] Badawi, A., Alharthi, S., Assaedi, H., Alharbi, A., Althobaiti, M. (2021), Cd0.9Co0.1S Nanostructures concentrated study on the structural and optical properties of the SWCNTs / PVA blend, Chem Phys Lett, 138701.

[9] Ali, B., Gaber, M., Abdallah, S., Johan, B., Mohammed, A., and Mohammed, A. (2021), Exploring the structural and optical properties of FeS filled graphene/ PVA blend for environmental-friendly applications, Journal of Polymer Research, 28, 1-12.

[10] Amita, S., Tamal, M., and Saswata, G. (2021), Fabrication of cellulose acetate nanocomposite films with lignocelluosic nanofiber filler for superior effect on thermal, mechanical and optical properties, Nano-Structures & Nano-Objects, 25.1-8.

[11] Mohamed, H., Abduelmajid, N. (2018), Optical Parameters of Polyvinyl Alcohol - Molybdenum Oxide Composite Films, Sciences (NWSAPS), 13(4),46-54.

[12] Atta, A., El-Nahass, M., Elsabawy, K., Abd El-Raheem, M., Hassanien, A., Al Huthali, A., Badawi, A.,and Merazga, A. (2016), Optical characteristics of transparent samarium oxide thin films deposited by the radio-frequency sputtering technique, Pramana, 87:72,1-8.

[13] Mostafa, N., Badawi, A., Ahmed, SI. (2018), Influence of Cu and Ag doping on structure and optical properties of In_2O_3 thin film prepared by spray pyrolysis,. Results in Physics, 10,126–131.

[14] Bouzidi, A., Omri, K., Jilani, W., Guermazi, H., Yahia, IS. (2018), Influence of TiO_2 Incorporation on the Microstructure, Optical, and Dielectric Properties of TiO_2/Epoxy Composites, J Inorg Organomet Polym Mater, 28,1114–1126.

[15] Abdullah, O., Aziz, S., Rasheed, M. (2016), Structural and optical characterization of PVA:$KMnO_4$ based solid polymer electrolyte, Results in Physics, 6,1103–1108.

[16] Badawi, A., Al-Gurashi, W., Al-Baradi, A., and Abdel-Wahab, F. (2020), Photoacoustic spectroscopy as a non-destructive technique for optical properties measurements of nanostructures, Optik, 201,1-23.

[17] Badawi, A., Al Otaibi, A., Albaradi, A., Al-Hosiny, N., Alomairy, S. (2018), Tailoring the energy band gap of alloyed Pb1− xZnxS quantum dots for photovoltaic applications, J Mater Sci Mater Electron, 29, 20914–20922.

[18] Tauc J. (1974). Amorphous and Liquid Semiconductors, 1st edition, Springer, Boston.p159-220.

[19] Badawi, A., Althobaiti, M. (2021), Effect of Cu-doping on the structure, FT-IR and optical properties of Titania for environmental- friendly applications, Ceram Int, 47,1389–1397.

[20] Shehap, A.and Dana, S. (2016), Structural and optical properties of TiO_2 nanoparticles/PVA for different composites thin films, Int. J. Nanoelectronics and Materials., **9**, 17-36.

[21] Wemple, S. and DiDomenico, M. (1971), Behavior of the electronic dielectric constant in covalent and ionic materials Phys. Rev., **B3**, 1338-1351.

[22] Omed, Gh., Yahya A. and Salwan A. (2015), In-situ Synthesis of PVA/HgS Nanocomposite Films and Tuning Optical Properties Phys. Mater. Chem., **3**, 18-24.

[23] Wug Dong park, Optical constant and Dispersion parameters of CdS Thin Film prepared by Chemical Bath Deposition, Transactions on Electrical and Electronic Materials 13(4), 2012, 196-199.

[24] Rashmi, ch., Amitkumar, S., Arvind, T., and Krishnakant, S. (2011), Linear and nonlinear optical changes in amorphous As2Se3 thin film upon UV exposure, Progress in Natural Science: Materials International, 21, 205-210.

[25] Taha, T., Hendawy, N., El-Rabaie, S., Asmaa, E., and El-Mansy, M. K. (2018), Effect of NiO NPs doping on the structure and optical properties of PVC polymer films, Polymer Bulletin, https://doi.org/10.1007/s00289-018-2633-2.

[26] Omed, Gh., Dlear, R. and Sherzad, A. (2015), The optical characterization of polyvinyl alcohol: cobalt nitrate solid polymer electrolyte films, Adv. Mater. Lett., **6**,153-157.

[27] El Sayed, A., El-Sayed, S., Morsi, W., Mahrous, S., and Hassen, A. (2014), Synthesis, characterization, optical, and dielectric properties of polyvinyl chloride/cadmium oxide nanocomposite films, Polym Compos, 35,1842–1851.

[28] Abdel-Baset, T., Elzayat, M., Mahrous, S. (2016), Characterization and optical and dielectric properties of polyvinyl chloride/silica nanocomposites films, Int J Polym Sci, 2016,1–10.

Ahmed, H. and Zinah, H. (2018), Synthesis, Characterization and Nanobiological Application of (Biodegradable Polymers-Titanium Nitride) Nanocomposites, Journal of Bionanoscience, 12, 504-507.